Technische Universität Berlin

Institut für Mathematik

A Multispecies Pedestrian Model based on a 3d multiphase incompressible fluid flow model

Tobias Ahnert **Günter Bärwolff** **Hartmut Schwandt**

Preprint 30-2012

Preprint-Reihe des Instituts für Mathematik
Technische Universität Berlin

Report 30-2012 **August 2012**

A Multispecies Pedestrian Model based on a 3d multiphase incompressible fluid flow model

Tobias Ahnert, Günter Bärwolff, and Hartmut Schwandt

TU Berlin, Institute of Mathematics, D-10623 Berlin, Str. d. 17. Juni 135, Germany

Abstract. The idea to simulate pedestrian flow by the application of fluid dynamics equations has a certain history in that field. This approach is based on the application of partial differential equations, which makes it a macroscopic method. The need to simulate several different species of pedestrians is a need from the start, which has not been matched very well by numerical simulations of the maroscopic type. The basis of the description of non dense pedestrian movement by incompressible fluid flow models consists in the introduction of an empty phase as a species of a multiphase system of distinct phases. In this article we describe the mathematical model and modifications to the multiphaseInterFoam-solver of the OpenFOAM library, which makes it applicable in this field and present results that show capabilities and limitations of the modified solver.

Keywords: pedestrian simulation; multiphase; incompressible flow

1 Introduction

The simulation of pedestrians is an important issue in transport and emergency applications. The current work in the field of pedestrian modelling and simulation can be roughly divided into micro- and macroscopic models. An overview of present results and models is given by Dogbe et al. [1].

One particular topic of interesst is the intersecting of pedestrian crowds, which occurs when path of pedestrian groups cross. Mircoscopic simulations for intersecting crowds are numberous and an example is the work by Helbing et al. [2].

For the simulation of intersecting crowds we tried several approaches from microscopic models (cf. Minjie Chen et al. [3]) to macroscopic models (cf. Berres et al. [4]) at our own research group. For evaluation purposes, video recordings of students crossing in a predefined area has been analysed by Plaue et al. [5].

The present article introduces a new technique for the simulation of several sepecies in macroscopic simulation of pedestrian crowds. The focus is on the modelling of several species with different destination and the ability to intersect each other rather than on a precise reconstruction of known pedestrian phenomena for prediction purposes. We proceed by first presenting the mathematical model followed by a concrete implementantion and some results. Based on the discussions in [6] and [7] we choose the incompressible Navier-Stokes equations

as a starting point of our model and added boundary conditions and transport equations to allow an intermixing and seperation of different species.

2 Mathematical Model

We use the non-stationary, incompressible Navier-Stokes equations

$$\begin{aligned} \rho\frac{\partial \boldsymbol{v}}{\partial t} + \rho\boldsymbol{v}\cdot\nabla\otimes\boldsymbol{v} + \nabla p - \\ \nabla\cdot(\mu(\nabla\otimes\boldsymbol{v}) + \mu(\nabla\otimes\boldsymbol{v})^T) = \boldsymbol{f} \\ \nabla\cdot\boldsymbol{v} = \boldsymbol{0} \end{aligned} \tag{1}$$

combined with a volume of fluid (VOF) method as a starting point to simulate $N_p \in \mathbb{N}$ different pedestrian species. Let $\mathbb{P} = \{1, \ldots, N_p\}$ be the set of indices of pedestrian groups, then the VOF method keeps track of the species' positions by introducing one fraction function per species

$$\alpha_i(\boldsymbol{x}) \in [0, 1],$$

that describes the fill level at position $\boldsymbol{x} \in \Omega$ of species $i \in \mathbb{P}$. The fraction function can be discontinuous, espeacially when discretized for implementation purposes. We demand the sum of all fraction functions to be one, i.e.

$$\sum_{i\in\mathbb{P}} \alpha_i = 1.$$

A standard VOF method uses the velocity computed by (1) with $\rho = \sum_{i\in\mathbb{P}} \rho_i\alpha_i$, $\mu = \sum_{i\in\mathbb{P}} \mu_i\alpha_i$ and changes every α_i by solving the transport equation

$$\frac{\partial \alpha_i}{\partial t} + \boldsymbol{v}\cdot\nabla\alpha_i = 0 \text{ for all } i \in \mathbb{P}. \tag{2}$$

In the course of pedestrian simulation we tried to simulate group crossing. Therefore, it was necessary to solve three modelling problems:

1. simulation of spaces without a pedestrian species
2. distinct species forces
3. seperation of species

2.1 Empty Spaces

An empty space is simulated by using a pedestrian group $f \in \mathbb{P}$, $\mathbb{P}_{\text{wf}} = \mathbb{P}\backslash\{f\}$. This so-called fill-species is able to leave Ω by flowing through an additional dimension, i.e. for a two-dimensional Ω the third dimension or z-axis. It is therefore necessary to simulate a three dimensional domain for a two dimensional problem.

The inflow and outflow over the third dimension is implemented using special boundary conditions that are aware of the fill-species. We used a solver that

is based on an operator splitting approach. Therefore, we have to choose two boundary conditions; one for the velocity and one for the pressure variable.

The boundary condition for the velocity is defined as

$$\begin{aligned} \boldsymbol{n}\cdot\boldsymbol{v} &= 0, \text{ for } \boldsymbol{n}\cdot\boldsymbol{\Phi} \geq 0, \alpha_f = 0 \\ \boldsymbol{n}\cdot\nabla(\boldsymbol{n}\cdot\boldsymbol{v}) &= 0 \text{ otherwise,} \end{aligned} \tag{3}$$

where $\boldsymbol{\Phi}$ is the velocity value adjacent to the boundary condition face from the last pressure correction step.

The pressure boundary condition is defined as

$$\begin{aligned} p &= \begin{cases} p_0 - \frac{1}{2}\rho\|\boldsymbol{v}\|^2, & \text{for } \boldsymbol{n}\cdot\boldsymbol{\Phi} < 0 \\ p_0, & \text{for } \boldsymbol{n}\cdot\boldsymbol{\Phi} \geq 0,\ \alpha_f > 0 \end{cases} \\ \boldsymbol{n}\cdot\nabla p &= 0, \text{ for } \boldsymbol{n}\cdot\boldsymbol{\Phi} \geq 0,\ \alpha_f = 0 \end{aligned} \tag{4}$$

on the z-axis. The other sides of the domain can be chosen as slip boundary conditions.

2.2 Species Forces

Each species of the intersection of pedestrians needs to have a distinct destination. Therefore the need to implement species specific forces and velocities arises. Each pedestrian species $i \in \mathbb{P}_{wf}$ has a desired velocity $\mathbf{v}_i^d$, that is the velocity a pedestrian species has without the influences of other pedestrian species.

The desired velocity gets transformed into a resulting force for the right hand side in the Navier-Stokes equation (1). Following the nomenclature by Helbing et al. for microscopic models (cf. [8], [9]), we introduce a so-called behavioural force

$$\mathbf{f} := C_2(\alpha^{bil})\Big(C_1(\alpha^{bil})\sum_{i\in\mathbb{P}_{\text{wf}}}\alpha_i\boldsymbol{v}_i^d - \boldsymbol{v}\Big), \tag{5}$$

with

$$\alpha^{bil} := \sum_{i\in\mathbb{P}_{\text{wf}}}\alpha_i$$

and add it to the right hand side of the Navier-Stokes equations (1). The functions C_1 and C_2 control the pedestrian behaviour, e.g. a choice of

$$\begin{aligned} C_1(\alpha^{bil}) &:= (1-\alpha^{bil}) \\ C_2(\alpha^{bil}) &:= \alpha^{bil} \end{aligned}$$

approximates the pedestrian fundamental diagram.

2.3 Seperation of Species

The seperation of species is not naturally given by the discretized VOF method. Equation (2) does not provide a mean of seperation of once mixed cells due to the fact we compute until now only a global velocity $\boldsymbol{v}$ out of the Navier-Stokes equations (1). Thus, we introduce an additional transport equation

$$\frac{\partial \alpha_i}{\partial t} - \nabla \cdot \left(C_3(\alpha_f) \frac{\boldsymbol{v}_i^d}{\|\boldsymbol{v}_i^d\|} \alpha_i \right) = 0 \tag{6}$$

for all $i \in \mathbb{P}_{\text{wb}}$ followed by

$$\alpha_f = 1 - \sum_{i \in \mathbb{P}_{\text{wf}}} \alpha_i \tag{7}$$

with C_3 defining the magnitude of the seperation velocity with a typical value of

$$C_3(\alpha_f) = \begin{cases} 0.01, & \text{for } \alpha_f > 0 \\ 0, & \text{for } \alpha_f = 0. \end{cases}$$

3 Implementation

We implemented the model by modifying the already available multiphaseInterFoam solver in OpenFOAM [10]. The multiphaseInterFoam solver uses the finite volume method (see for a reference of finite volume methods [11]) for the incompressible Navier-Stokes equations and further implements the VOF method for multiphase simulations. The Navier-Stokes equation is solved using the so-called Pressure Implicit with Splitting Operators (PISO) algorithm [12]. The solver consists mainly of three distinct steps. The velocity predictor step, the pressure correction loop and the fraction function adjustments. It further implements a surface tension force, which has been disabled for our experiments, but might be used in combination with our model, too.

We need to introduce some notation to proceed. We will call $\mathcal{E}$ the set of all velocity nodes and $\mathcal{N}(i), i \in \mathcal{E}$ the set of all neighbor nodes of i, that is the nodes whose cell share a face with the cell of i. Let us denote by V_i the volume of a cell for node $i \in \mathcal{E}$.

3.1 The velocity predictor step

Let ρ_g and μ_g be defined as

$$\rho_g = \sum_{i \in \mathbb{P}} \rho_i \alpha_i, \quad \mu_g = \sum_{i \in \mathbb{P}} \mu_i \alpha_i,$$

where μ_i and ρ_i are species dependend and $\mathbf{f}$ be computed by (5). For the most simple case we use the explicit Euler method, so equation (1) becomes

$$\int_{V_i} \rho_g \frac{\boldsymbol{v}^{n+1} - \boldsymbol{v}^n}{\Delta t} \,\mathrm{d}\boldsymbol{x} + \int_{\partial V_i} (\boldsymbol{n} \cdot \rho_g \boldsymbol{\Phi}^n)\boldsymbol{v}^n \,\mathrm{d}\boldsymbol{s} + \int_{V_i} \nabla p^n \,\mathrm{d}\boldsymbol{x} - \int_{V_i} \nabla \cdot (\mu_g(\nabla \otimes \boldsymbol{v}^n) + \mu_g(\nabla \otimes \boldsymbol{v}^n)^T) \,\mathrm{d}\boldsymbol{x} = \int_{V_i} \boldsymbol{f}^n \,\mathrm{d}\boldsymbol{x} \tag{8}$$

in a finite volume context, where $\boldsymbol{\Phi}$ is the velocity interpolated to the faces using the values from neighbor cells and n symbolizes the current time step. OpenFOAM is using a kind of Rhie-Chow interpolation for flux fields, which we will symbolize by Π.

Then the algebraic equation for a single cell $i \in \mathcal{E}$ of (8) becomes

$$a_i \boldsymbol{v}_i + \sum_{n \in \mathcal{N}(i)} a_n \boldsymbol{v}_n = \boldsymbol{b}_i - \nabla p_i \tag{9}$$

in discretized form, where $a_i \in \mathbb{R}$ are the coefficients for $\boldsymbol{v}_i$ and $\boldsymbol{b}$ represents the right hand side of the algebraic equation without the pressure.

3.2 The pressure correction loop

Let A be the diagonal matrix containing all a_i from equation (9), that is for $k = \lfloor j/3 \rfloor$ let $(A)_{jj} = a_k$ and $(A)_{ij} = 0$ for $i \neq j$ and further let H be the vector containing all $a_n \boldsymbol{v}_n$ and the right hand side $\boldsymbol{b}_i$, that is

$$H_{3i+j} = (-\sum_{n \in \mathcal{N}(i)} a_n \boldsymbol{v}_n + \boldsymbol{b}_i)_j \text{ for } j \in \{1, 2, 3\}.$$

This H-operator is common for OpenFOAM based implementations. We then compute a Jacobi step for $\mathbf{v}$ with

$$\boldsymbol{v}_{\text{jac}} = A^{-1} H$$

Next, we compute $\boldsymbol{\Phi} = \Pi(\boldsymbol{v}_{\text{jac}} + A^{-1}\boldsymbol{f})$ followed by

$$\nabla \cdot (A^{-1} \nabla p^{n+1}) = \nabla \cdot \boldsymbol{\Phi} \tag{10}$$

to compute the new p^{n+1}.

The face flux Φ is then corrected by

$$\Phi^{n+1} = \Pi(A^{-1}H - A^{-1}\nabla p)$$

followed by the correction of the velocity

$$\boldsymbol{v}^{n+1} = \boldsymbol{v}_{\text{jac}} - \nabla p.$$

The boundary conditions (3) and (4) are used for the z-axis in equations (1) and (10), respectively. The velocity's boundary conditions have been set to slip at non-penetratable walls and boundary conditions for the pressure have been chosen as zero gradient. The pressure correction loop is repeated until the pressure converges or a maximum number of rounds is reached.

3.3 Adjustment of the Fraction Function

The computation of $\boldsymbol{v}^{n+1}$ allows the adjustment of the fraction function via (2). It follows the seperation of the species by solving (6) and (7). Usually a downwind scheme should be used for the evaluation of C_3, so it is set depending on the α_f value in the target cell.

When the fraction function has been adjusted, the velocity predictor step continues with the next time step.

4 Numerical Results

We produced simulation results for quadratic geometries with an orthogonal mesh and on a more complex geometry inspired by real world experiments in the Technical University of Berlin [5].

Table 1 shows the results for a quadratic area with two species crossing in 180 degrees.

As can be seen from table 1 the species cross each other, show stripe formation, create lanes and reach their desination on opposite walls. At the end of the simulation the species are completely seperated. It should, however, be noted, there are several effects originating in the impuls conservation, which are rather unnatural for crowd simulation. For example the the occurence of a splash at the moment the species hit a wall with larger values of $\boldsymbol{v}$, which is due to the impuls conservation and can be seen at time $T = 20.0$ in table 1. There, one is able to see species one splashing back at the bottom wall. Further, the masses have a non-neglectable acceleration time, which is in contrast to pedetrians behaviour.

Table 2 shows the results for a quadratic area with two species crossing in 90 degrees. As for the 180 degrees example both species cross, seperate and reach their destination. Impuls effects again play a big role in the simulation, since generally the bigger mass wins and squeezes the smaller mass out of their way. Another effect is the acceleration of a small mass due to squeezing by a much larger mass, which is also unnatural for pedestrians.

We made real world experiments, that can be used to test parameters and validate the numerical results. In 2010 and 2011 we performed several experiments with up to four crowd groups that were crossing in a predefined area. The experiments have been recorded on video and we were able to observe common crowd phenomena like lane formation and isolated groups (c.f. [5]). It also allowed us to get quantitative results for evaluation purposes by video analysis [5].

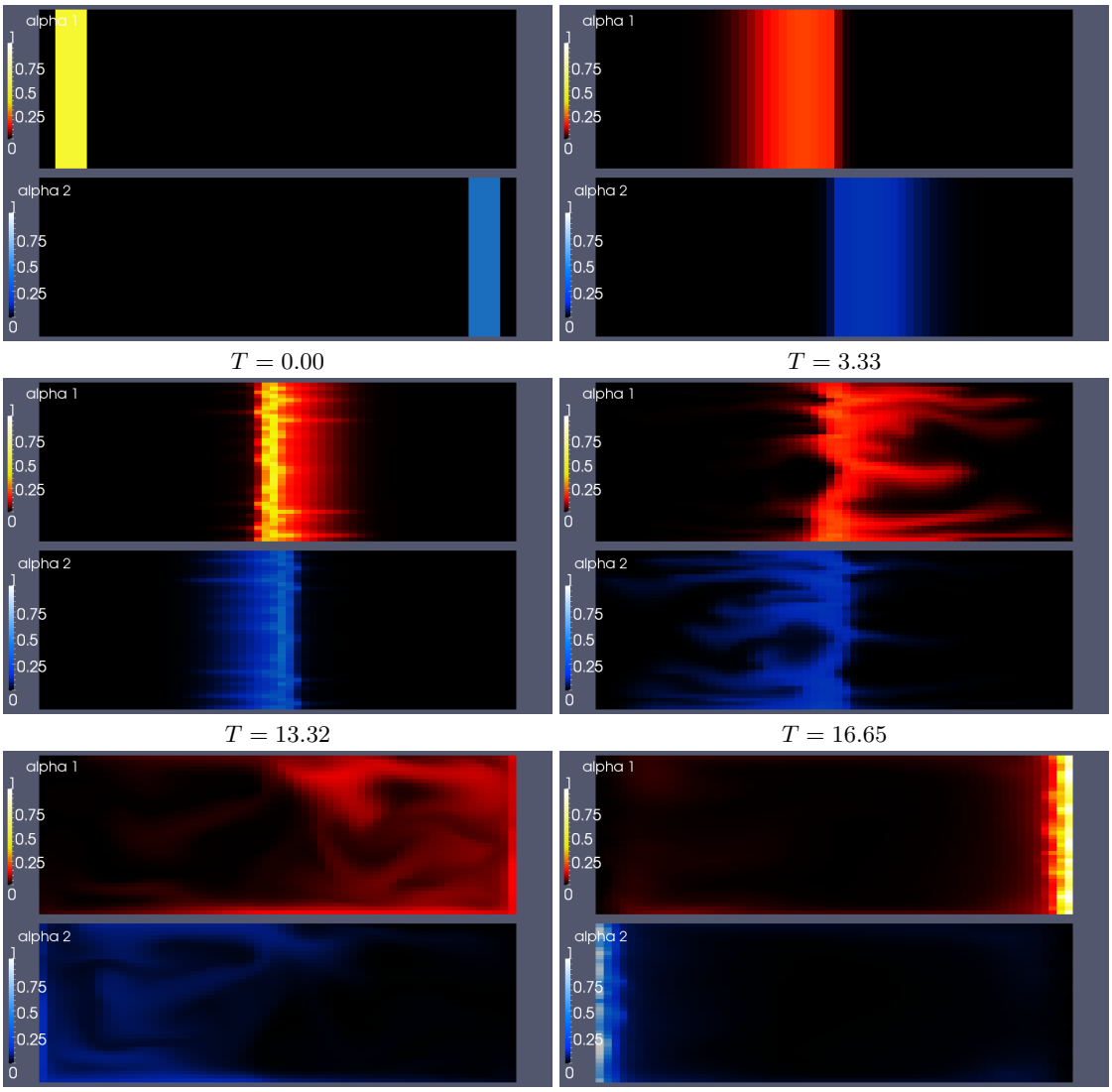

$T = 0.00$ $T = 3.33$

$T = 13.32$ $T = 16.65$

$T = 20.00$ $T = 30.00$

Table 1. Simulation of 180 degress crossing with $\max(\boldsymbol{u}) = 10.0$, $\boldsymbol{v}_{ps} = 0.04$, $\max(F_{bil}) = 1000$ as parameters.

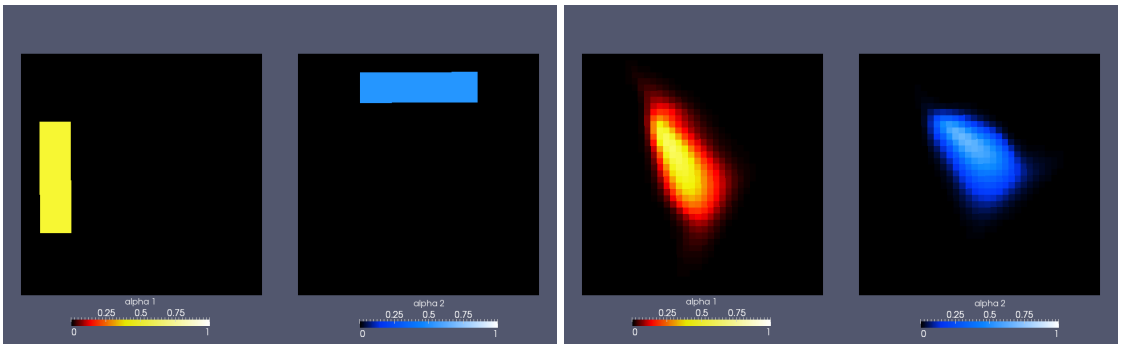

$T = 0.00$ $T = 2.78$

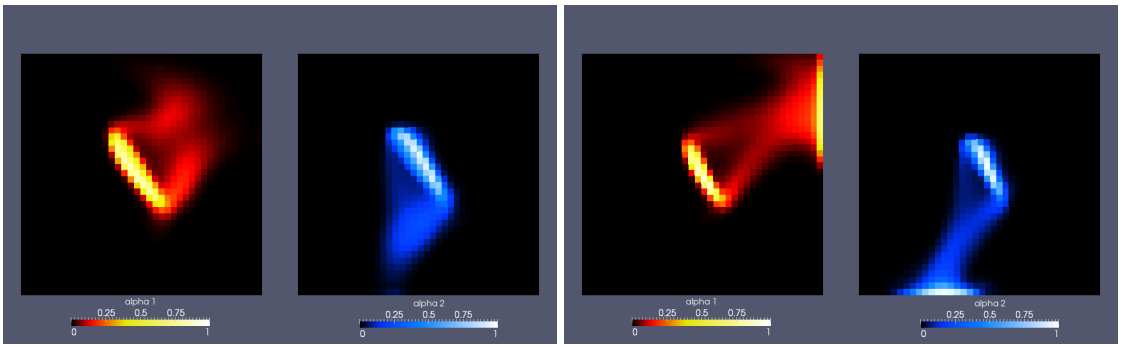

$T = 5.56$ $T = 8.34$

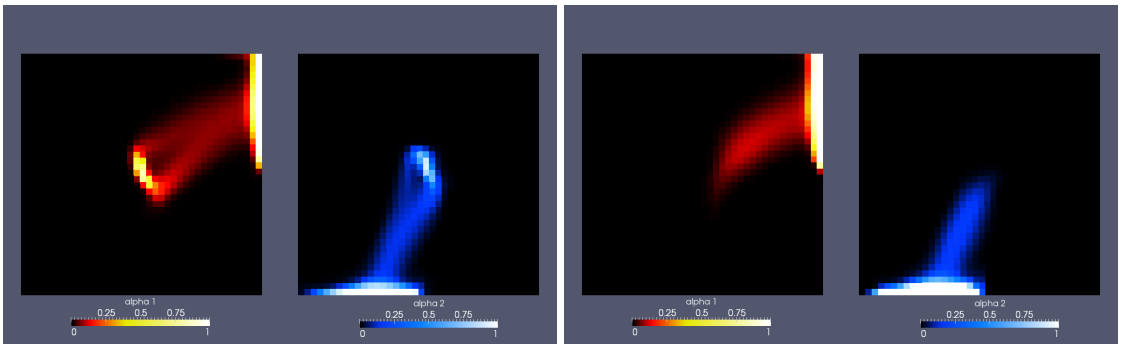

$T = 11.12$ $T = 13.89$

Table 2. Simulation of 90 degress crossing with $\max(\boldsymbol{u}) = 1.0$, $\boldsymbol{v}_{ps} = 0.1$, $\max(F_{bil}) = 1000$ as parameters.

Therefore, we made numerical simulation on a mesh with a geometry similar to the control area in the real world experiments. The simulation in the control area shows lane formation and congestions before an entrance, see picture 1. The origin of the congestions lays in the very static desired velocities we are currently using. A more dynamical desired velocity that better models pedestrian long and short sight behaviour is subject of future work.

Experiments showed the fill-species and the pedestrian species should have the same density ρ. Otherwise, we may create artificial impulses through the seperation step that could move heavier species to a place with higher velocity. Although different ρ values for different species will work, the impuls bilance should be kept in mind.

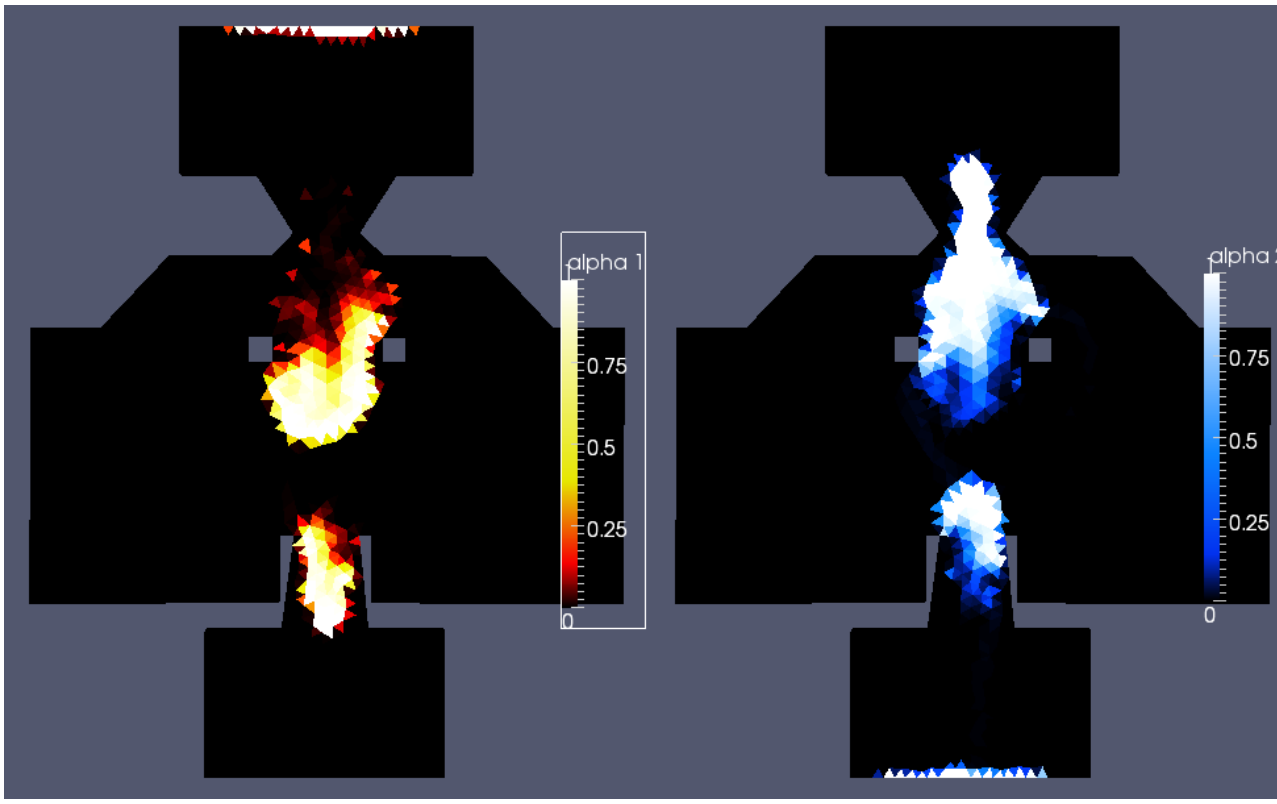

Fig. 1. Simulation done with a complex geometry inspired by real world experiments.

We were also able to implement very basic in- and outlet boundary conditions for multiple species, i.e. the fill-species and a pedestrian species. For inlet boundaries we use a fixed value condition for the velocity together with the pressure boundary condition 4. For outlet boundary conditions we use 4 and 3

for the pressure and velocity, respectively. Further research should be put in in- and outlet boundary conditions for more complex in- and outflow scenarios of pedestrian, e.g. the rate of flow should be controlable depending on the fill rate of cells next to the inlet boundary.

5 Discussion

We presented a new ansatz for the simulation of pedestrian crossing and multi-species simulation. The implementation is based on the incompressible Navier-Stokes equations with a volume of fluid ansatz that has been altered by special boundary conditions for the pressure and the velocity as well as an added transport equation for the seperation of intermixed species. The proposed model allowed us to reproduce common pedestrian crossing effects like stripe and lane formation. It also allows us to simulate higher numbers (more than two) of pedestrian species.

The model showed impuls effects originating from the Navier-Stokes equations, which are unnatural for pedestrian behaviour. Therefore, it is the subject of future work to use a different set of equations and to study the stability and conservation properties of the solver in more detail. Another topic is the implementation of open boundaries for the in- and outflow of pedestrians in the simulation.

6 Acknowledgment

The authors were funded by the Institut fr Mathematik, Technische Universitt Berlin through the DFG project “Methods for modeling and large-scale simulation of multi-destination pedestrian crowds”.

References

1. Bellomo N, Dogbe C. On the Modeling of Traffic and Crowds: A Survey of Models, Speculations, and Perspectives. SIAM Review. 2011;53(3):409–463. Available from: http://link.aip.org/link/?SIR/53/409/1.
2. Helbing D, Buzna L, Johansson A, Werner T. Self-Organized Pedestrian Crowd Dynamics: Experiments, Simulations, and Design Solutions. Transportation Science. 2005 February;39:1–24. Available from: http://dl.acm.org/citation.cfm?id=1247226.1247227.
3. Chen M, Brwolff G, Schwandt H. A study of step calculations in traffic cellular automaton models. In: Intelligent Transportation Systems (ITSC), 2010 13th International IEEE Conference on; 2010. p. 747 –752.
4. Schwandt H, Berres S. A Simulation Model for Two-phase Pedestrian Flow. AIP Conference Proceedings. 2011;1389(1):1825–1828. Available from: http://link.aip.org/link/?APC/1389/1825/1.

5. Plaue M, Chen M, Brwolff G, Schwandt H. Trajectory Extraction and Density Analysis of Intersecting Pedestrian Flows from Video Recordings. In: Stilla U, Rottensteiner F, Mayer H, Jutzi B, Butenuth M, editors. Photogrammetric Image Analysis. vol. 6952 of Lecture Notes in Computer Science. Springer Berlin / Heidelberg; 2011. p. 285–296. 10.1007/978-3-642-24393-6_24. Available from: http://dx.doi.org/10.1007/978-3-642-24393-6_24.
6. Brwolff G, Slawig T, Schwandt H. Modeling of Pedestrian Flows Using Hybrid Models of Euler Equations and Dynamical Systems. AIP Conference Proceedings. 2007;936(1):70–73. Available from: http://link.aip.org/link/?APC/936/70/1.
7. Henderson LF. The Statistics of Crowd Fluids. Nature. 1971 Feb;229(5284):381–383. Available from: http://dx.doi.org/10.1038/229381a0.
8. Helbing D, Molnár P. Social force model for pedestrian dynamics. Phys Rev E. 1995 May;51:4282–4286. Available from: http://link.aps.org/doi/10.1103/PhysRevE.51.4282.
9. Johansson A, Helbing D, Shukla P. Specification of the social force pedestrian model by evolutionary adjustment to video tracking data. Advances in Complex Systems. 2007;(10):271–288.
10. OpenFOAM 1.7.x. The OpenFOAM Foundation; 2011. Available from: http://www.openfoam.org.
11. Ferziger JH, Peri M. Computational methods for fluid dynamics. 3rd ed. Springer; 2002.
12. Issa RI. Solution of the implicitly discretised fluid flow equations by operator-splitting. Journal of Computational Physics. 1986;(62).